Molecules and Cells

Recombinant Human HAPLN1 Mitigates Pulmonary Emphysema by Increasing TGF-β Receptor I and Sirtuins Levels in Human Alveolar Epithelial Cells

Yongwei Piao[1,2], So Yoon Yun[1,2], Zhicheng Fu[1], Ji Min Jang[1], Moon Jung Back[1], Ha Hyung Kim[1], and Dae Kyong Kim[1,2,*]

[1]Department of Environmental & Health Chemistry, College of Pharmacy, Chung-Ang University, Seoul 06974, Korea, [2]HaplnScience Inc., Seongnam 13494, Korea
*Correspondence: kimdk@haplnscience.com
https://doi.org/10.14348/molcells.2023.0097
www.molcells.org

Chronic obstructive pulmonary disease (COPD) will be the third leading cause of death worldwide by 2030. One of its components, emphysema, has been defined as a lung disease that irreversibly damages the lungs' alveoli. Treatment is currently unavailable for emphysema symptoms and complete cure of the disease. Hyaluronan (HA) and proteoglycan link protein 1 (HAPLN1), an HA-binding protein linking HA in the extracellular matrix to stabilize the proteoglycan structure, forms a bulky hydrogel-like aggregate. Studies on the biological role of the full-length HAPLN1, a simple structure-stabilizing protein, are limited. Here, we demonstrated for the first time that treating human alveolar epithelial type 2 cells with recombinant human HAPLN1 (rhHAPLN1) increased TGF-β receptor 1 (TGF-β RI) protein levels, but not TGF-β RII, in a CD44-dependent manner with concurrent enhancement of the phosphorylated Smad3 (p-Smad3), but not p-Smad2, upon TGF-β1 stimulation. Furthermore, rhHAPLN1 significantly increased sirtuins levels (i.e., SIRT1/2/6) without TGF-β1 and inhibited acetylated p300 levels that were increased by TGF-β1. rhHAPLN1 is crucial in regulating cellular senescence, including p53, p21, and p16, and inflammation markers such as p-NF-κB and Nrf2. Both senile emphysema mouse model induced via intraperitoneal rhHAPLN1 injections and porcine pancreatic elastase (PPE)-induced COPD mouse model generated via rhHAPLN1-containing aerosols inhalations showed a significantly potent efficacy in reducing alveolar spaces enlargement. Preclinical trials are underway to investigate the effects of inhaled rhHAPLN1-containing aerosols on several COPD animal models.

Keywords: alveolar epithelial type 2 cells, extracellular matrix, pulmonary emphysema, recombinant human HAPLN1, senescence, TGF-β receptor I

INTRODUCTION

According to the World Health Organization, chronic obstructive pulmonary disease (COPD) will be the third leading cause of death worldwide by 2030 (Murray and Lopez, 2013). COPD is characterized by chronic bronchitis, small airway remodeling, and emphysema (Königshoff et al., 2009) and mainly affects older adults as an accelerated lung aging disease (Barnes, 2017). The hallmark of emphysema includes alveolar structures destruction, leading to enlarged air spaces and reduced surface area. Experimental evidence suggests that emphysema development is driven by accelerated senescence of lung cells; however, the underlying mechanism of senescence remains unknown (Mercado et al., 2015). COPD is a chronic inflammatory lung disease, and inflammation has

Received June 8, 2023; revised June 22, 2023; accepted June 24, 2023; published online August 17, 2023

eISSN: 0219-1032

been indicated as crucial in the early stages of emphysema, considering the earliest alveolar destruction mechanism (Mebratu et al., 2016). Therefore, it is generally accepted that cellular senescence and inflammation are intertwined in accelerated or premature lung aging (inflammaging) (Rahman et al., 2012).

Nevertheless, a recent study interestingly showed that inhibiting lung inflammation using the selective nuclear factor (NF)-κB/IKK2 inhibitor PHA-408 did not affect cellular senescence or emphysematous destruction (Yao et al., 2012). This observation suggests that NF-κB–dependent lung inflammation does not fully account for such lung dysfunction or that it is possibly a cellular senescence consequence. The observation also demonstrated sirtuin 1 (SIRT1) deficiency causing early emphysema development in an elastase-induced emphysema animal model and cigarette smoke (CS)-induced COPD mouse model. Senescence has been shown to negatively correlate with the expression and activity of SIRT1, a protein deacetylase that protects against DNA damage and cellular senescence (Paschalaki et al., 2013). In this context, down-regulated SIRT1 was reported in the lungs of smokers or patients with COPD (Rajendrasozhan et al., 2008), and co-activator-associated arginine methyltransferase-1 (CARM1)-deficient mice have recently been shown to reduce a basal level of SIRT1-positive alveolar epithelial cells (Sarker et al., 2015). Subsequent experiments revealed that CARM1 deficiency also leads to low SIRT1-positive airway epithelial cells level with concurrent increases in p16- and p21-positive cell basal levels in COPD pathogenesis, implying its role in epithelial senescence upstream of SIRT1 (Sarker et al., 2019). Among sirtuins, SIRT1 and SIRT6 are the best protectors against vascular aging (D'Onofrio et al., 2018) and COPD (Mercado et al., 2015) through the prevention of cellular senescence and inflammation by regulating both phosphorylated NF-κB (p-NF-κB) and nuclear factor erythroid 2-related factor 2 (Nrf2).

Reactive oxygen species (ROS) formed during normal oxygen metabolism induce damage and ROS accumulation accounts for progressive deleterious changes called aging or senescence (Harman, 2006). This increase in ROS deposition is also a feature in COPD lungs and aged tissue, causing DNA damage. Antioxidant enzyme activity is also known to be decreased in COPD (Kirkil et al., 2008). Cellular senescence and the inhibition of antioxidant genes are evident in COPD, which is known to be regulated by sirtuins (Baker et al., 2016; Nakamaru et al., 2009). Currently, over 200 Nrf2-driven genes are exploited for detoxification and antioxidant defense (Zhang et al., 2013), clarifying the active search for more effective antioxidants and a particular interest in developing drugs that will activate or restore Nrf2 activity, which is impaired in COPD cells (Mercado et al., 2015).

Phosphorylated Smad3 (p-Smad3), a key element in the canonical transforming growth factor β (TGF-β) pathway, exerts a positive regulatory impact on neonatal lung alveolarization, potentially protecting the lungs against future centrilobular emphysema via inhibition of metalloproteinase-9 (MMP9), which leads to an early onset destructive emphysema phenotype (Chen et al., 2005). Consistently, TGF-β appears to be crucial in protecting the hyperoxic alveolar epithelial type 2 cells against *in vitro* and *in vivo* oxidative damage through Smad signaling (Buckley et al., 2008; Warburton et al., 2013).

We previously discovered hyaluronan and proteoglycan link protein 1 (HAPLN1) as a protein associated with skin aging using surgically anastomosed parabiotic mice and the aptamer-based proteomic analysis of their blood proteins. HAPLN1 has been known to non-covalently link and strongly stabilize numerous proteoglycans onto the hyaluronan (HA) backbone, forming a water-rich, bulky, and bottle-brush-like complex. The complex is termed HAPLN1-containing aggregate, and can maintain tissues structural integrity including skin and lung tissues, by anchoring to CD44 receptors on cell surfaces. HA is a linear heteropolysaccharide, usually presented as a large molecular weight polymer (1,000-2,000 kDa), one of the main components of the extracellular matrix (ECM) (Garantziotis and Savani, 2019). HA can form ECM when binding to the major cell receptor CD44 (Sorokin, 2010). In some stress conditions, high molecular weight HA (HMW-HA) are rapidly degraded by ROS, hyaluronidase enzymes, and mechanical forces to produce pro-inflammatory low molecular weight HA (LMW-HA) fragments (<250 kDa), known as damage-associated molecular patterns, serving as ligand molecules for CD44 and other receptors such as Toll-like receptors (Jiang et al., 2005). The resultant LMW-HA are removed from tissues by endocytosis upon formation of such HA-CD44 receptor complexes (Misra et al., 2015).

Furthermore, similar to integrin signaling, HA-CD44 interactions have been shown to transfer information from the ECM directly by themselves and indirectly by associated signaling molecules linked to their cytoplasmic domain (Isacke and Yarwood, 2002). Therefore, blocking or reducing the rate of CD44 endocytosis may prevent the degradation of a larger complex composed of the aggregates, CD44, and various associated molecules like TGF-β receptors. Our recent study demonstrated for the first time that full-length recombinant human HAPLN1 (rhHAPLN1) selectively increased the levels of TGF-β receptor II (TGF-β RII) reduced by an endocytic degradation in a CD44-dependent manner in normal human dermal fibroblasts and subsequently led to the concomitant enhancement in gene expressions of pro-collagen I and HA synthase 2. Human alveolar epithelial type 2 cells (HAEC2), which may be the progenitors of type 1 cells (HAEC1), show senescence in COPD (Barkauskas et al., 2013), are capable of self-renewal, and normally become activated by hyperoxic injury or damage to HAEC1 resulting in re-epithelialization of the lung (Desai et al., 2014).

Interestingly, in contrast to our previous study, we demonstrated that treating HAEC2 with rhHAPLN1 increased TGF-β RI, but not TGF-β RII, in a CD44-dependent manner with simultaneous enhancement of p-Smad3 form, but not p-Smad2. Consequently, our results indicated that such CD44-dependent and selective increase in p-Smad3 levels lead to an increase in SIRT1 levels, and therefore revealed that rhHAPLN1 exerted significantly beneficial effects on cellular senescence and inflammation markers including p53, p21, p16, p-NF-κB, and Nrf2, in the *in vitro* COPD mimicking settings induced by cell-damaged insults such as porcine pancreatic elastase (PPE), H_2O_2, IL-1β, and LMW-HA. Furthermore, in both senile and PPE-induced COPD mouse emphysema

models, intraperitoneal rhHAPLN1 injections and inhaled rhHAPLN1-containing aerosols administrations showed an extremely potent efficacy in reducing alveolar spaces enlargement.

MATERIALS AND METHODS

Animals

Twenty-month-old male C57BL/6J mice were purchased from Korea Basic Science Institute (Korea). Six-week-old male C57BL/6J mice were purchased from Samtako BioKorea Inc. (Korea). Pathogen-free, 8-week-old male C57BL/6N mice were purchased from Orient Bio Inc. (Korea). The animals were housed under specific pathogen-free conditions and in an environment of 22°C ± 2°C and relative humidity of 50% ± 5%, with 12 h/12 h of light/dark cycle. All animal experiments were performed according to the National Research Council's Guidelines for Animal Experiments of Chung-Ang University and approved by the university committee for animal experiments (IACUC No. 201800103).

rhHAPLN1 preparation by cell culture and purifications

The DNA encoding full sequence of human HAPLN1 was transfected in CHO-K1 host cells. The transfected CHO-K1 cell culture was performed using bioreactor in fed-batch mode. The culture medium was harvested by depth filtration to remove the host cells and debris from the culture medium. Purification was performed through several chromatography steps to make high purity rhHAPLN1 protein. The purity was 96.5%, as determined using size exclusion-high-performance liquid chromatography, and the concentration of the endotoxin was 0.05 EU/mg. The purified rhHAPLN1 was 2.0 mg/ml in 20 mM sodium acetate (pH 5.0) and stored at −70°C until use. The purified rhHAPLN1 showed approximately 80% of link protein 1 (LP1) at 48 kDa and approximately 20% of link protein 2 (LP2) at 44 kDa, respectively, by sodium dodecyl sulfate-polyacrylamide gel electrophoretic (SDS-PAGE) analysis under reducing conditions (Roughley et al., 1982) (Supplementary Fig. S1).

Study on alveolar and lung function in old mice

Five young male C57BL/6J mice of 6 to 10 weeks and two groups of five old male mice of 19 to 20 months were used. Young mice and one group of old mice were treated with phosphate-buffered saline (PBS) as control groups. One group of the old mice was intraperitoneally injected with rhHAPLN1 of 0.1 mg/kg in PBS once every three days for a total of nine times and then euthanized after a day of the final injection. The young mice or vehicle control group received an intraperitoneal injection of PBS. The lungs were harvested, parasagittal sectioned, immersed in formalin, and built into paraffin blocks. The lung tissues were cut into 5 μm and stained with H&E.

Study on alveolar and lung function in emphysema-induced mice

Male C57BL6/N mice aged eight weeks were used as experimental materials and divided into four groups: normal (N), control (C), rhHAPLN1 (HapInScience Inc.), and hyaluronic acid (HA). To induce emphysema, PPE (30 μl/6 Units/time/animal) was injected into the oral airway with a 0.9 mm × 50 mm-oral zonde as a method of aerosol inhalation (AH) a day before exposure to the test samples, and the test samples were treated from the second day. rhHAPLN1 (3.3 μg/ml and 5.0 μg/ml, 10 ml) were exposed for 1 h inside Mass Dosing Nebulizing Chamber (Data Sciences International, USA). The mice were exposed to saline for the control group, 0.0005% (5×10^{-4}%, w/v) for each group of rhHAPLN1, and 0.005% (5×10^{-3}%, w/v) HA (>2,500 kDa) for the HA group for 1 h each time and five times per week for two weeks in the chamber, and then euthanized after one day of the final exposure. The experiment used a mass-dosing nebulizing chamber with the mass-dosing aerosol controller (Harvard Bioscience, USA) to control the nebulization and generate aerosols. The nebulizer was connected to a heavy-duty air compressor that delivered a constant pressure of 30 psi. The aerosol entered the exposure chamber through an inflow port attached to the roof and was drawn through the chamber by negative pressure created by a vacuum pump connected to an exhaust port on the side wall. The chamber was large enough (18 × 12 × 11 inches) to permit the mice to remain in their cages while inhaling the aerosol, thereby minimizing the direct handling of the animals (Cantor et al., 2005).

Histological examinations

The formalin-fixed samples were decalcified, embedded in paraffin, and sectioned. The sections were stained with H&E as previously described (Liu et al., 2019). Sample preparation was outsourced to the Korea Pathology Technical Center (Korea).

Cell culture of primary human alveolar epithelial cells (HAECs)

All the culture media and additives used in the HAECs culture were purchased from Cell Biologics (USA). HAECs were also provided by Cell Biologics. HAECs were cultured for expansion in Human Epithelial Cell Medium Supplement Kit. The medium consists of 500 ml of basal medium (containing essential and non-essential amino acids, vitamins, organic and inorganic compounds, hormones, growth factors, and trace minerals), supplemented with epithelial cell growth supplement, 1% antibiotics, and 5% fetal bovine serum. The cells were cultured in Complete Human Epithelial Cell Medium (CHECM; Cell Biologics) at 37°C in a 5% CO_2 humidified incubator. HAECs were subcultured when the culture reached 80% confluency or above. The cells were detached with 0.05% Trypsin/EDTA solution and centrifuged at 1,000 rpm for 3 min. HAECs were resuspended with CHECM and seeded in gelatin-based coating solution coating T75 flask cell culture dishes at a density of 1,000,000 cells.

Western blotting

HAECs were seeded in gelatin-coating 6-well plates at a density of 1.0×10^5 cells per well and incubated for 24 h at 37°C with 5% CO_2. A complete medium replaced the medium, and the HAECs were stimulated with TGF-β1 (5 ng/ml), IL-1β (20 ng/ml), LMW-HA 15 to 30 kDa (1 μg/ml), and H_2O_2 (300 μM). The HAECs were subsequently treated with rhHAPLN1

(25 ng/ml) and incubated for 23 h at 37°C with 5% CO_2. The cells were harvested and sonicated with the lysis buffer (25 mM Tris-HCl, 1 mM EDTA, 0.1% Triton-X100, phosphatase inhibitor, and protease inhibitor cocktail). The protein concentrations of the lysates were determined using the BCA protein assay kit (Pierce Biotechnology, USA) using bovine serum albumin (BSA) as a standard. Equal amounts of whole protein extracts were separated on acrylamide gels using SDS-PAGE. SDS-PAGE was performed with 15 μg protein, which was successively transferred to polyvinylidene fluoride (PVDF) membrane (Bio-Rad, USA) and incubated overnight at 4°C with specific primary antibodies, namely TGF-β RI, TGF-β RII, CARM1, SIRT6 (Abcam, UK), SIRT1, p53, p21, p16, MMP9, GAPDH (Santa Cruz Biotechnology, USA), SITR2, Samd2/3, p-Smad2, p-Smad3, p300, Ac-p300, Nrf2, NF-κB, p-NF-κB, and CD44 (Cell Signaling Technology, USA) at a dilution of 1:2,000. The membranes were then individually washed thrice in TBST (25 mM Tris-HCl, 130 mM NaCl, 2.5 mM KCl, 0.1% Tween 20) for 5 min, and incubated for 1.5 h at room temperature (24°C) with secondary HRP-conjugated antibodies (Cell Signaling Technology) which were used to visualize protein expression levels as the signal intensity on light-exposed X-ray film. The protein bands were developed by ECL (Femto; GenDEPOT, USA) solution. Protein was checked using FUSION FX (Vilber, France).

DCFDA-cellular transfection and flow cytometry measurement of ROS

Intracellular ROS levels were evaluated using a 2′-7′-dichlorofluorescein diacetate (DCFDA) fluorescent probe (GeneCopoeia, USA). HAECs were seeded in gelatin-coating 6-well plates at a density of 1.5×10^5 cells per well and incubated for 24 h at 37°C with 5% CO_2. The cultured cells were divided into 10 groups: non-stained control, control stained with DCFDA, and treated with IL-1β, LMW-HA, PPE, and H_2O_2 with or without rhHAPLN1 followed by DCFDA staining. Cells were harvested and the single-cell suspension was ensured using accutase; harvested cells were centrifuged at 1,000 rpm for 3 min. Furthermore, 0.5 ml of 20 μM DCFDA solution diluted 1:10 with PBS containing 1% BSA and 1 mM EDTA was added, and the cells were incubated for 30 min at 37°C in the dark. After 30 min, they were centrifuged at 1,000 rpm for 3 min, the supernatants were discarded, and 200 μl of PBS containing 1% BSA and 1 mM EDTA solution was added to the e-tubes and resuspended. Forward and side scatter (FSC and SSC, respectively) gates were established to exclude debris and cellular aggregates from the analysis. DCFDA was excited using the 488 nm laser and detected at 535 nm (typically FL1). Ideally, 10,000 cells should be analyzed per experimental condition.

Small interfering RNA (siRNA) transfection

CD44- and CARM1-specific and non-specific control siRNA (Santa Cruz Biotechnology) into HAECs at a final concentration of 200 pmol using jetPRIME complying with the manufacturer's instruction. The transfected cells were utilized following 6 h of transfection. Knockdown was confirmed by western blotting.

Statistics

All the results are expressed as the mean ± SEM and analyzed using the IBM SPSS software (ver. 23.0; IBM, USA). Statistical significance was set at $*P < 0.05$ and high significance at $**P < 0.01$, $***P < 0.001$. $^{\#}P < 0.05$ and high significance at $^{\#\#}P < 0.01$, $^{\#\#\#}P < 0.001$.

RESULTS

Type analysis and verification of HAECs by fluorescence activated cell sorting (FACS)

The HAECs used in the experiments could be a mix of HAEC1 and HAEC2. Therefore, the types of cells need to be first identified by intercellular staining (Creative Bioarray, USA). HOPX, Pdpn, and Ager were used as cell-specific markers for HAEC1, and surfactant protein C (SP-C) (Santa Cruz Biotechnology) was used as a cell-specific marker for HAEC2, considered adult stem cell-like cells (Jain et al., 2015; Rodriguez-Castillo et al., 2018). Rabbit-FITC staining was performed and the stained cells were detected using FACS flow cytometry; 94.4% of the HAECs were identified as HAEC2 (Supplementary Fig. S2).

rhHAPLN1 induces selective increases in TGF-β RI and p-Smad3 levels with concurrent increases in SIRT1 and p300 and decreases in MMP9 and Ac-p300 levels

TGF-β signaling is crucial in lung development, injury, and repair through p-Smad3–mediated SIRT1 expression (Warburton et al., 2013). We hypothesized a positive role of rhHAPLN1 in this TGF-β signaling and thus first detected the levels of TGF-β receptors by western blotting. Our data showed that rhHAPLN1 at 50 ng/ml rhHAPLN1 significantly increased the levels of TGF-β RI but not TGF-β RII (Fig. 1A). In contrast, the observations that CD44, a major receptor for HA, is known to associate directly with TGF-β receptors at the cell surface (Bourguignon et al., 2002; Harada and Takahashi, 2007) intrigued an investigation of the effects of rhHAPLN1 and/or exogenous HA on the increase in TGF-β RI levels, revealing an approximately doubled increase and no synergistic effect or change in the levels of TGF-β RI even by treating with both rhHAPLN1 and exogenous HA (Fig. 1B). As addressed above, as p-Smad3–mediated TGF-β signaling was reported to cooperate with c-Jun to regulate a protein deacetylase SIRT1 synergistically, we next analyzed rhHAPLN1-induced increases in Smad2 and Smad3 levels and their phosphorylation upon TGF-β1 stimulation.

Interestingly, our results showed that rhHAPLN1 enhanced p-Smad3 levels, shortly increased by TGF-β1 stimulation (Fig. 1C). Therefore, it is likely that rhHAPLN1 promotes the TGF-β-p-Smad3 signaling axis, which was shown to result in the regulation of SIRT1 and MMP9 expressions, namely increases in SIRT1 as well as decreases in MMP9 levels (Warburton et al., 2013). Accordingly, our data indicated that treating HAEC2 cells with rhHAPLN1 increased SIRT1 levels and reduced MMP9 levels via rapid signaling independent of TGF-β1 stimulation (Fig. 1C), suggesting that such changes may result from post-transcriptional changes in their levels along with the p-Smad3–mediated transcriptional expression. In addition, it has been demonstrated that activation of SIRT1

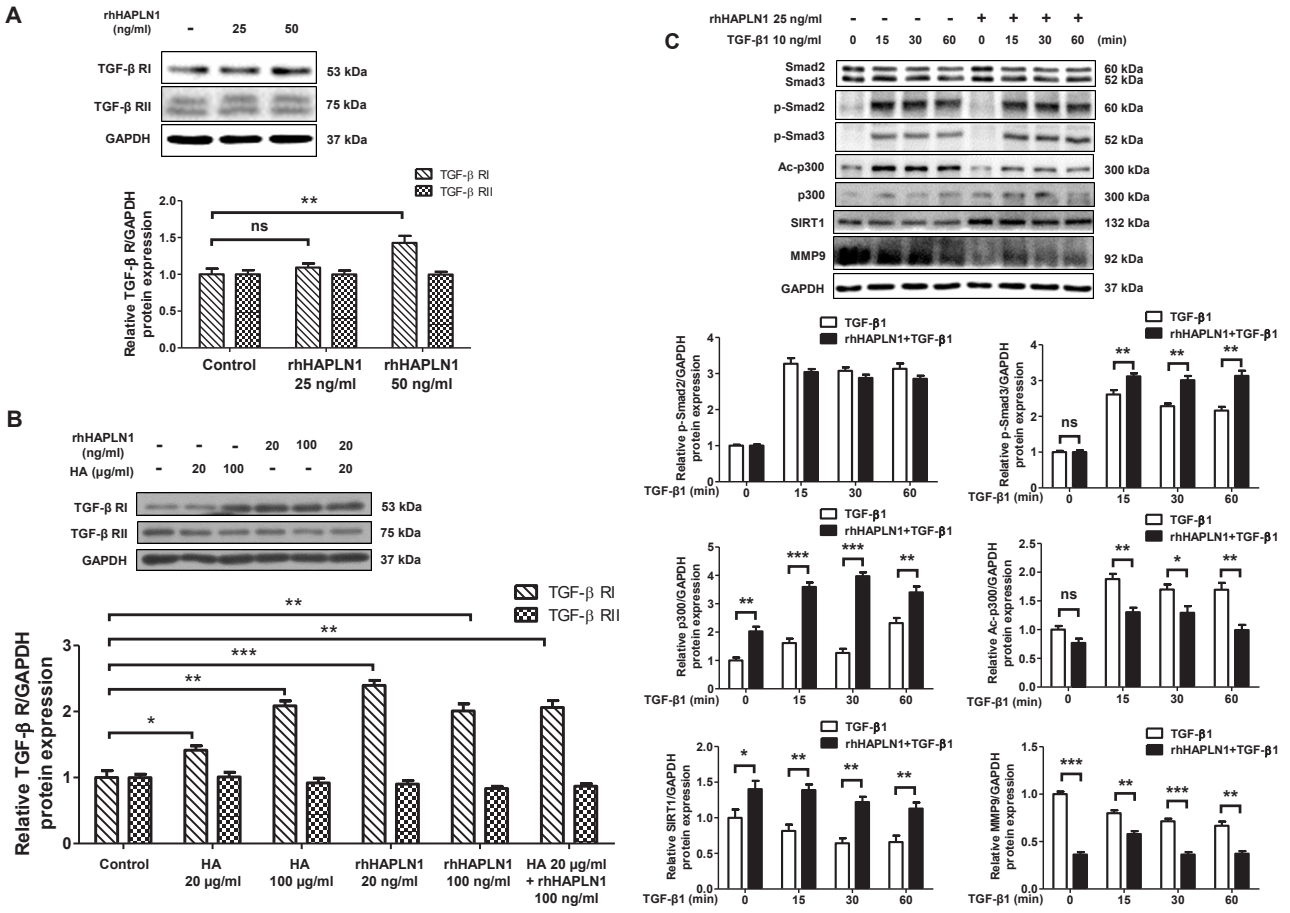

Fig. 1. rhHAPLN1 induces selective increases in TGF-β RI and p-Smad3 levels with concurrent increases in SIRT1 and p300 and decreases in MMP-9 and Ac-p300 levels. Human alveolar epithelial cells (HAECs) (Passage 15) cells were seeded at 1 × 10^5 cells/6-well plate culture with CHECM (Cell Biologics). Protein levels were analyzed by western blotting as described in Materials and Methods section. (A) rhHAPLN1 (25 and 50 ng/ml) was treated for 24 h. (B) HAECs were treated with rhHAPLN1 (20 and 100 ng/ml) and/or HA (>2,500 kDa) (20 and 100 μg/ml) at the indicated concentrations for 24 h in serum-free condition. (C) At 24 h after rhHAPLN1 treatment, TGF-β1 (10 ng/ml) was treated for 0, 15, 30, and 60 min. The protein levels of TGF-β RI, TGF-β RII, Smad2/3, p-Smad2, p-Smad3, Ac-p300, p300, SIRT1, MMP9, and GAPDH were determined by western blotting. Protein samples (15 μg per lane) were loaded for immunoblot as described in Materials and Methods section. The results (mean ± SEM) represent three independent experiments (n = 3). $*P < 0.05$, $**P < 0.01$, $***P < 0.001$ versus Control or non-rhHAPLN1 group. ns, no significance. rhHAPLN1, recombinant human hyaluronan and proteoglycan link protein 1; TGF-β RI, transforming growth factor β receptor 1; p-Smad3, phosphorylated Smad3; SIRT1, sirtuin 1; MMP9, metalloproteinase-9; Ac-p300, acetylated p300.

by resveratrol induces inactivation of p300 acetyltransferase by SIRT1 via SIRT1-p300 association; deacetylation of the active form of acetylated p300 (Ac-p300). Therefore, we tested the rhHAPLN1-induced changes in the levels of p300, which is known to be an enzyme that inhibits or competes with the deacetylating ability of SIRT1. Our results showed that Ac-p300 levels were significantly reduced by treating rhHAPLN1 (Fig. 1C). The precise mechanism involved in HA-CD44-linked p300 signaling has not been established; however, these data suggest that rhHAPLN1 may play an important role in upregulating SIRT1 levels.

Rescue effects of rhHAPLN1 on decreases in TGF-β RI, SIRT1/2/6, and CARM1 levels induced by cell-damaging insults, and its ROS scavenging effects

CS-induced oxidative stress has been shown to reduce SIRT1 levels in lung tissue of COPD patients (Kato et al., 2016). It has also been shown that CARM1 deficiency attenuates SIRT1-regulated anti-aging, thereby inducing alveolar epithelial cell aging and increased susceptibility to elastase-induced emphysema (Sarker et al., 2019). To investigate whether rhHAPLN1 can protect HAECs damaged by various insults, including PPE and H_2O_2, we first treated the cells with PPE and found the reduced levels of TGF-β RI, SIRT1, and CARM1 in a dose-dependent manner (Supplementary Fig. S3) (Hou et al., 2013; Liang and He, 2019). Our results showed that

PPE-stimulated downregulation of TGF-β RI, SIRT1, SIRT2, SIRT6, and CARM1 levels was significantly reversed by the treatment with rhHAPLN1 (Fig. 2A), implying the possible protection against the PPE-induced HAECs destruction and senescence through CARM1-SIRT1 axis. To further confirm the anti-aging effect of rhHAPLN1 in HAECs, we performed knockdown experiments using siCARM1 (CARM1 siRNA). The results showed that SIRT1 and SIRT6 were significantly reduced in response to siCARM1 (Supplementary Fig. S4A). Sirtuins have been shown to exert a pro-longevity effect in some insects and mammals when the expression levels of sirtuins, especially SIRT1, SIRT2, and SIRT6, are increased (Yu et al., 2021). Contrastingly, it has been shown that H_2O_2-induced ROS production increases cellular senescence significantly (Zhu et al., 2021). Our results revealed that the siNC group increased both SIRT1/6 and Nrf2 levels by rhHAPLN1. In contrast, the siCARM1 group did not exert such increases in both (Fig. 2B), suggesting that CARM1 may act upstream of SIRT1 and prevent the production of ROS or have its scavenging role similar to the previous study (Barnes, 2017; Sarker et al., 2015). In this regard, it should be noted that Nrf2 expression was reduced in patients with COPD, thus

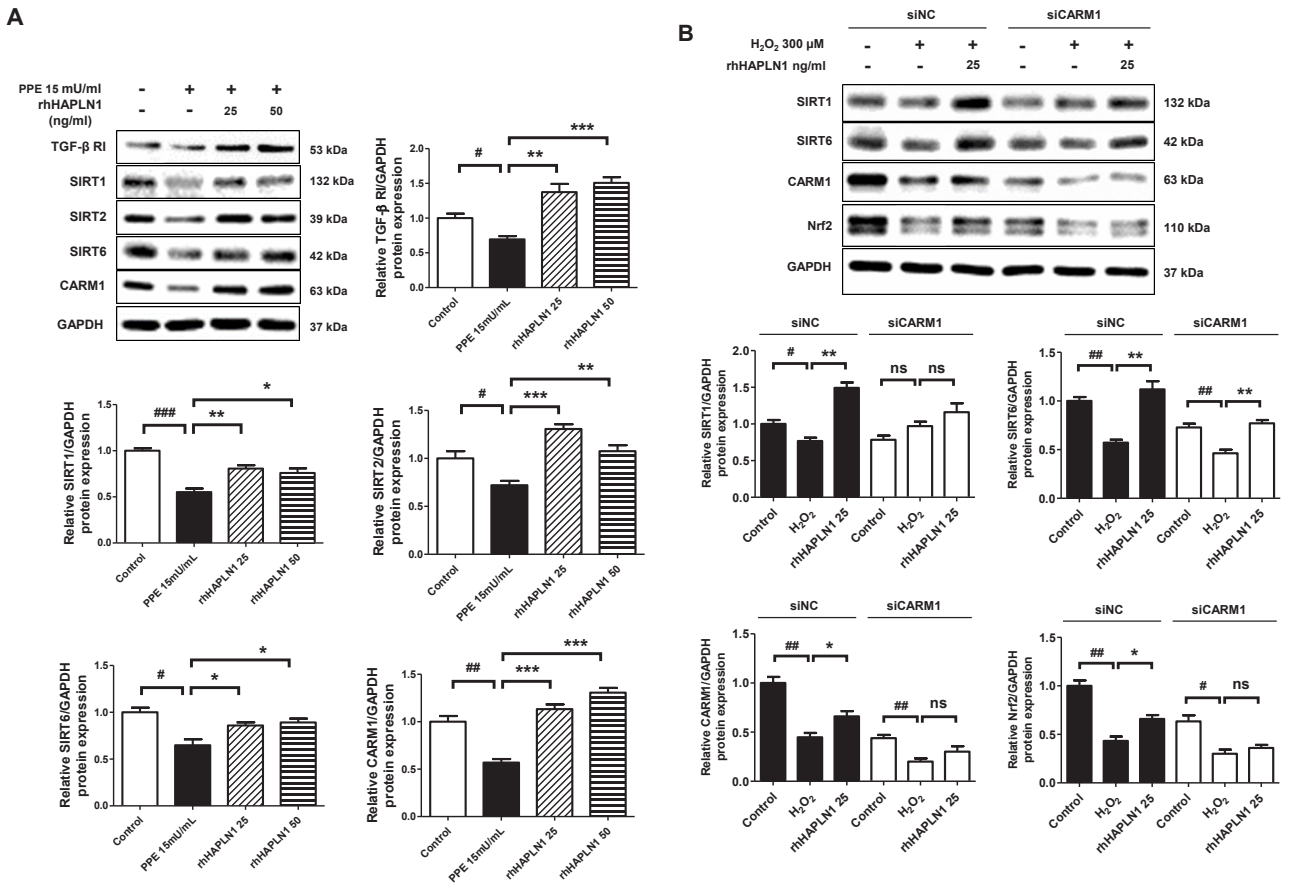

Fig. 2. Rescue effects of rhHAPLN1 on protein levels of TGF-β RI, SIRT1/2/6, and CARM1 reduced by cell-damaging insults, and its ROS scavenging effects. Human alveolar epithelial cells (HAECs) (Passage 3) were seeded at 1 × 10^5 cells/6-well plate culture with CHECM (Cell Biologics). (A) At 24 h after porcine pancreatic elastase (PPE) (15 mU/ml) pretreatment, rhHAPLN1 (25 and 50 ng/ml) was treated for 24 h. The levels of TGF-β RI, SIRT1, SIRT2, SIRT6, CARM1, and GAPDH were analyzed by western blotting as described in Materials and Methods section. (B) HAECs (Passage 16) were transfected with either siNC or siCARM1 with CHECM. At 5 h after CARM1 siRNA pretreatment, CHECM was replaced with a complete medium for 19 h. At 24 h after CARM1-knockdown, following pretreatment of 300 μM H_2O_2 for 1 h, rhHAPLN1 (25 ng/ml) was treated for 24 h. (C) HAECs (Passage 3) were exposed to 300 μM H_2O_2, 15 mU/ml PPE, 20 ng/ml IL-1β, and 1 μg/ml LMW-HA for 1 h and incubated for 24 h in the presence or absence of rhHAPLN1. ROS was measured as the fluorescence intensity of DCFDA using FACS. (D) HAECs were treated with rhHAPLN1 (25 and 50 ng/ml) at the indicated concentrations for 24 h in serum-free conditions. (E) At 1 h after PPE (15 mU/ml) pretreatment, rhHAPLN1 (25 and 50 ng/ml) was treated for 24 h. The protein levels of TGF-β RI, SIRT1, SIRT2, SIRT6, CARM1, Nrf2, p53, p21, p16, and GAPDH were determined by western blotting. Protein samples (15 μg of protein per lane) were loaded for immunoblot as described in Materials and Methods section. The results (mean ± SEM) represent three independent experiments (n = 3). $^{\#}P < 0.05$, $^{\#\#}P < 0.01$, $^{\#\#\#}P < 0.001$ versus Control. $*P < 0.05$, $**P < 0.01$, $***P < 0.001$ versus positive Control (insults treatments). ns, no significance. rhHAPLN1, recombinant human hyaluronan and proteoglycan link protein 1; TGF-β RI, transforming growth factor β receptor 1; SIRT1, sirtuin 1; CARM1, co-activator-associated arginine methyltransferase-1; ROS, reactive oxygen species.

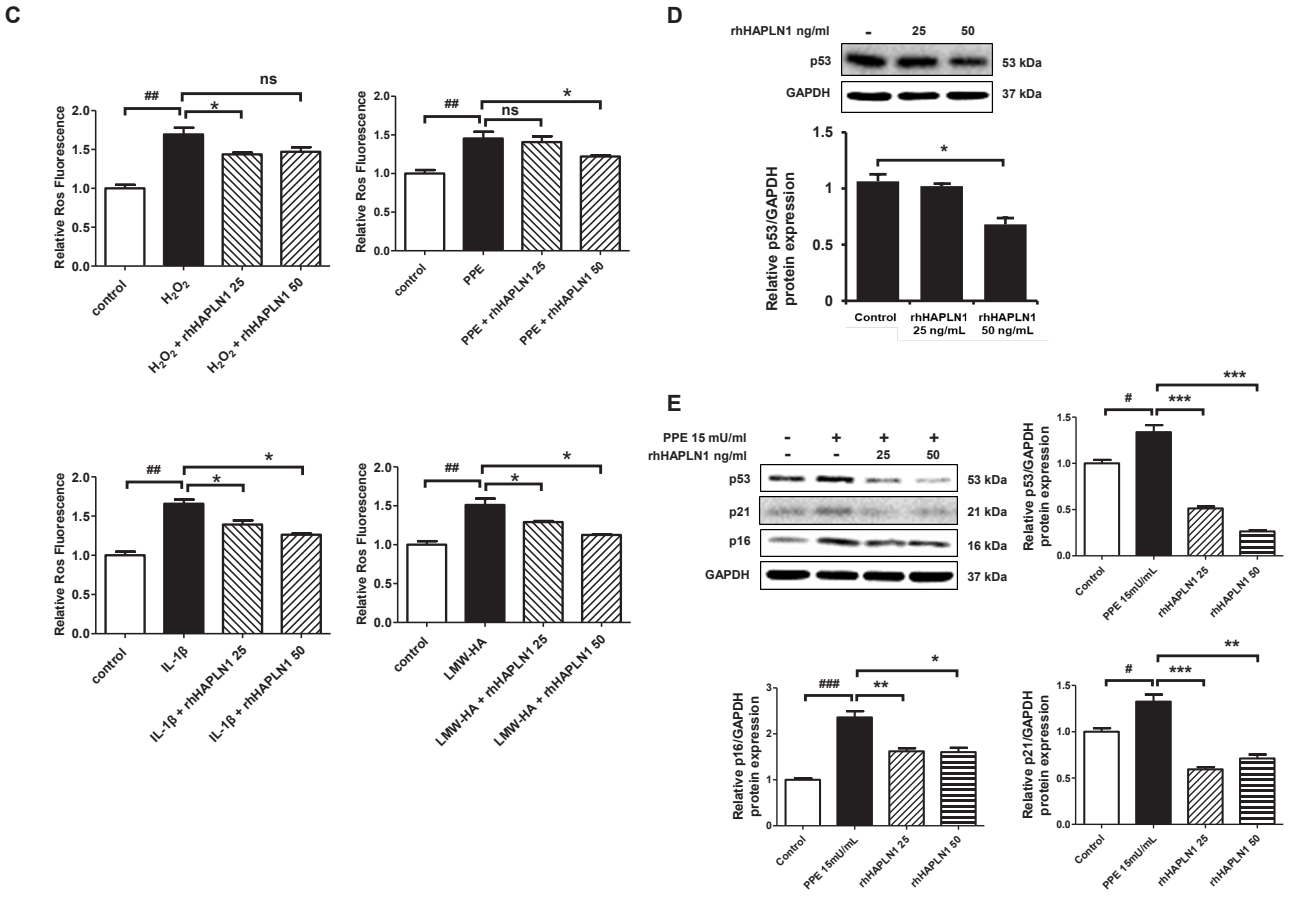

Fig. 2. Continued.

weakening the expression of Nrf2-driven cell protective genes (Vomund et al., 2017). Furthermore, we demonstrated the effects of rhHAPLN1 on the scavenging of ROS produced by H_2O_2, PPE, IL-1β, and LMW-HA, which are considered critical inflammatory factors released during COPD. The results indicated significant effects of rhHAPLN1 on ROS scavenging (Fig. 2C). Finally, such ROS scavenging effects of rhHAPLN1 led us to investigate whether rhHAPLN1 can prevent cellular senescence induced by tumor suppressors like p53, thus revealing that rhHAPLN1 suppressed p53 levels in HAECs (Fig. 2D). Furthermore, our study expanded to indicate that the siCARM1 group showed increased levels of p53, p21, and p16 as the markers of cell cycle arrest and cellular senescence compared with the siNC group (Supplementary Fig. S4B). Next, our PPE-induced COPD model established in HAECs revealed enhanced p53, p21, and p16 levels, and such enhancements were significantly reduced by rhHAPLN1 (Fig. 2E). In particular, p53 has been suggested to play a central role in SIRT1-mediated functions in tumorigenesis, senescence, and beyond (Yi and Luo, 2010). Our data highlight that rhHAPLN1 rescues the levels of SIRT1/2/6, CARM1, and Nrf2 downregulated in HAECs exposed to several damaging insults through the increased levels of TGF-β RI at the cell surface. Additionally, it should be noted that rhHAPLN1 reduced p53 levels in resting cells and suppressed p53, p21, and p16 upregulated in PPE-stimulated cells.

rhHAPLN1 not only failed to increase the levels of TGF-β RI but also failed to reverse decreases in the levels of TGF-β RI, SIRT1, and SIRT6 induced by cell-damaging insults in CD44-knockdown HAECs

HA is known to regulate TGF-β RI through CD44 (Harada and Takahashi, 2007; Ouhtit et al., 2013). Therefore, CD44 is considered an important factor in the role of rhHAPLN1 in regulating TGF-β RI levels at the cell surface. To verify such involvement of CD44 in the increased TGF-β RI levels induced by rhHAPLN1, we transfected the HAECs with CD44 siRNA. We prepared the cells by reducing them by approximately 50% in 83-kDa standard forms of CD44 (Supplementary Fig. S5). Treatment of CD44 siRNA-transfected HAECs with rhHAPLN1 resulted in a poor restoration of TGF-β RI levels compared with those in the siNC group (Fig. 3A), suggesting that such poor rescue of the decreased TGF-β RI levels may be due to the low levels of CD44. In contrast, interestingly, the low levels of CD44 due to CD44 siRNA also resulted in poor restoration of p-NF-κB levels by rhHAPLN1 (Fig. 3A). Notably, our findings that rhHAPLN1 downregulates p-NF-κB and upregulates SIRT1 and SIRT6 in a CD44-dependent manner highlight its anti-inflammation as well as anti-senescence functions in COPD pathogenesis. However, notably, our results showed

that H_2O_2-induced elevation of p-NF-κB levels was reversed by rhHAPLN1. Such elevation was promoted rather than reversed under the knockdown of CD44 (Fig. 3B), suggesting that rhHAPLN1 exerted H_2O_2-induced enhancement of p-NF-κB levels regardless of CD44; however, it may affect p-NF-κB levels through a factor or pathway different from TGF-β RI and SIRT1/6 pathways. Next, we investigated the link between cell-damaged insults, including IL-1β and LMW-HA, and the rescue effect of rhHAPLN1. Our results indicated that the downregulation of TGF-β RI induced by IL-1β and not LMW-HA was rescued by rhHAPLN1 regardless of CD44. Contrastingly, the downregulation of TGF-β RI and SIRT1/6 induced by IL-1β and LMW-HA were rescued by rhHAPLN1 CD44-dependently (Figs. 3C and 3D).

Intraperitoneal administration of rhHAPLN1 significantly suppresses enlarged alveolar spaces of aged mice

During aging, lung function progressively worsens, and the lung space becomes structurally enlarged despite the lack of alveolar wall destruction, termed senile emphysema, which is also accompanied by pulmonary inflammation (Ito and Barnes, 2009). Furthermore, previous studies interestingly indicated that COPD patients showed excessive skin wrinkling compared with normal smokers (Patel et al., 2006) and that reduction in SIRT1 as an anti-aging molecule caused such a structural change in the lung (Yanagisawa et al., 2017). Along with these studies and our *in vitro* data on the sirtuins, we examined the pathological conditions of alveoli in lung tissue after intraperitoneal administration of rhHAPLN1 of 0.1 mg/kg in PBS once every three days for a total of nine times. Thereafter, we euthanized mice after 1 day of the final

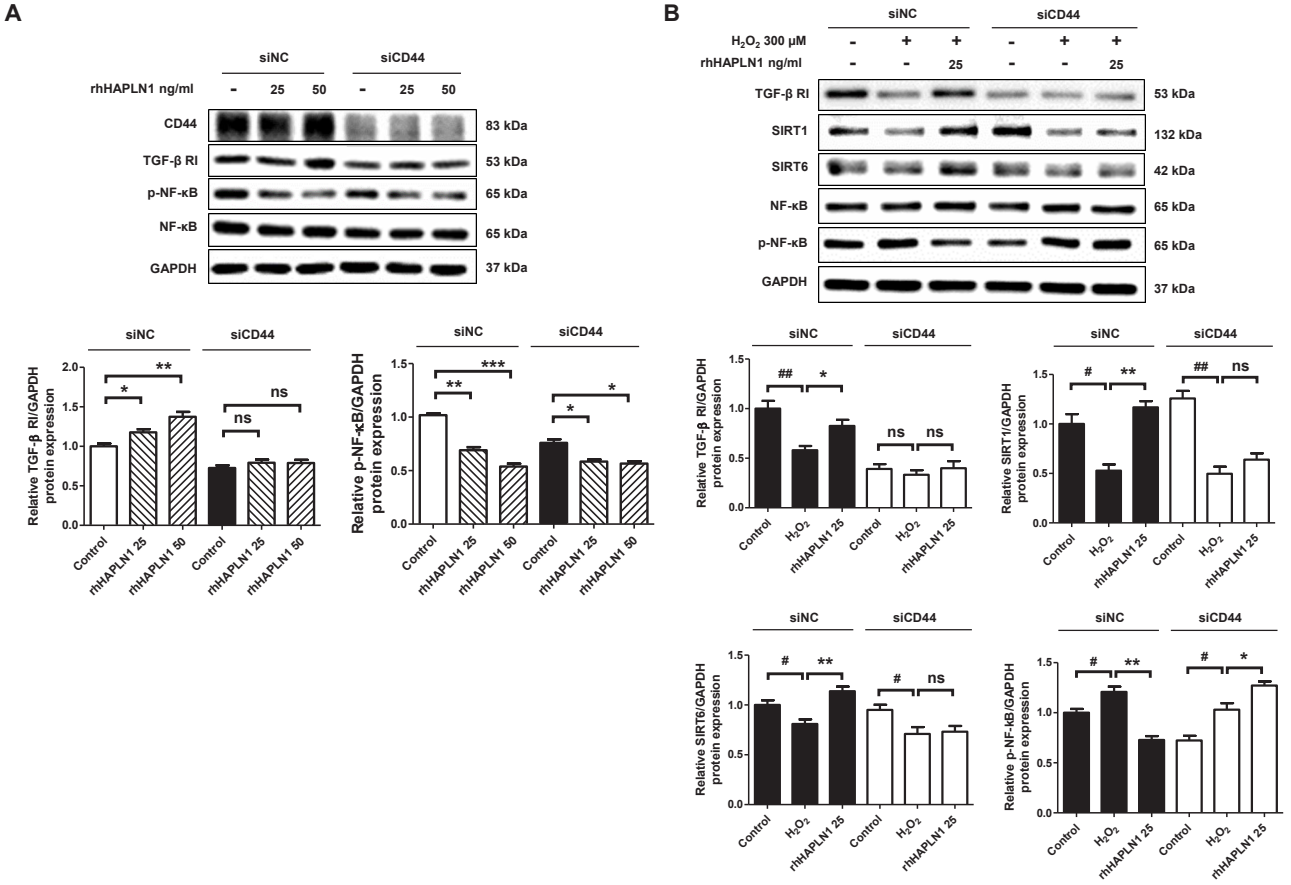

Fig. 3. The effects of CD44 deficiency on the levels of TGF-β RI, SIRT1/2/6, and p-NF-κB in various cell-damaging insults-exposed HAECs, and rescue effects exerted by rhHAPLN1. HAECs (Passage 13) were seeded at 1 × 10^5 cells/6-well plate culture with CHEM (Cell Biologics). At 4 h after CD44 siRNA pretreatment, CHECM was replaced with a complete medium for 20 h. (A) rhHAPLN1 (25 and 50 ng/ml) were treated for 24 h. In addition, to test the reversal effects of rhHAPLN1 on such changes in levels induced by cell-damaging insults, at 24 h after the CD44-knockdown, H_2O_2 300 μM (B), IL-1β 20 ng/ml (C), and low molecular weight hyaluronan (LMW-HA) 1 μg/ml (D) were pre-treated for 1 h, followed by rhHAPLN1 (25 ng/ml) treatment for 24 h. The protein levels of CD44, TGF-β RI, SIRT1, SIRT6, NF-κB, p-NF-κB, and GAPDH were determined by western blotting. Protein samples (15 μg per lane) were loaded for immunoblot as described in Materials and Methods section. The results (mean ± SEM) represent three independent experiments (n = 3). $^{\#}P < 0.05$, $^{\#\#}P < 0.01$, $^{\#\#\#}P < 0.001$ versus Control. $*P < 0.05$, $**P < 0.01$, $***P < 0.001$ versus positive Control (insults treatments). ns, no significance. TGF-β RI, transforming growth factor β receptor 1; SIRT1, sirtuin 1; p-NF-κB, phosphorylated NF-κB; HAECs, human alveolar epithelial cells; rhHAPLN1, recombinant human hyaluronan and proteoglycan link protein 1.

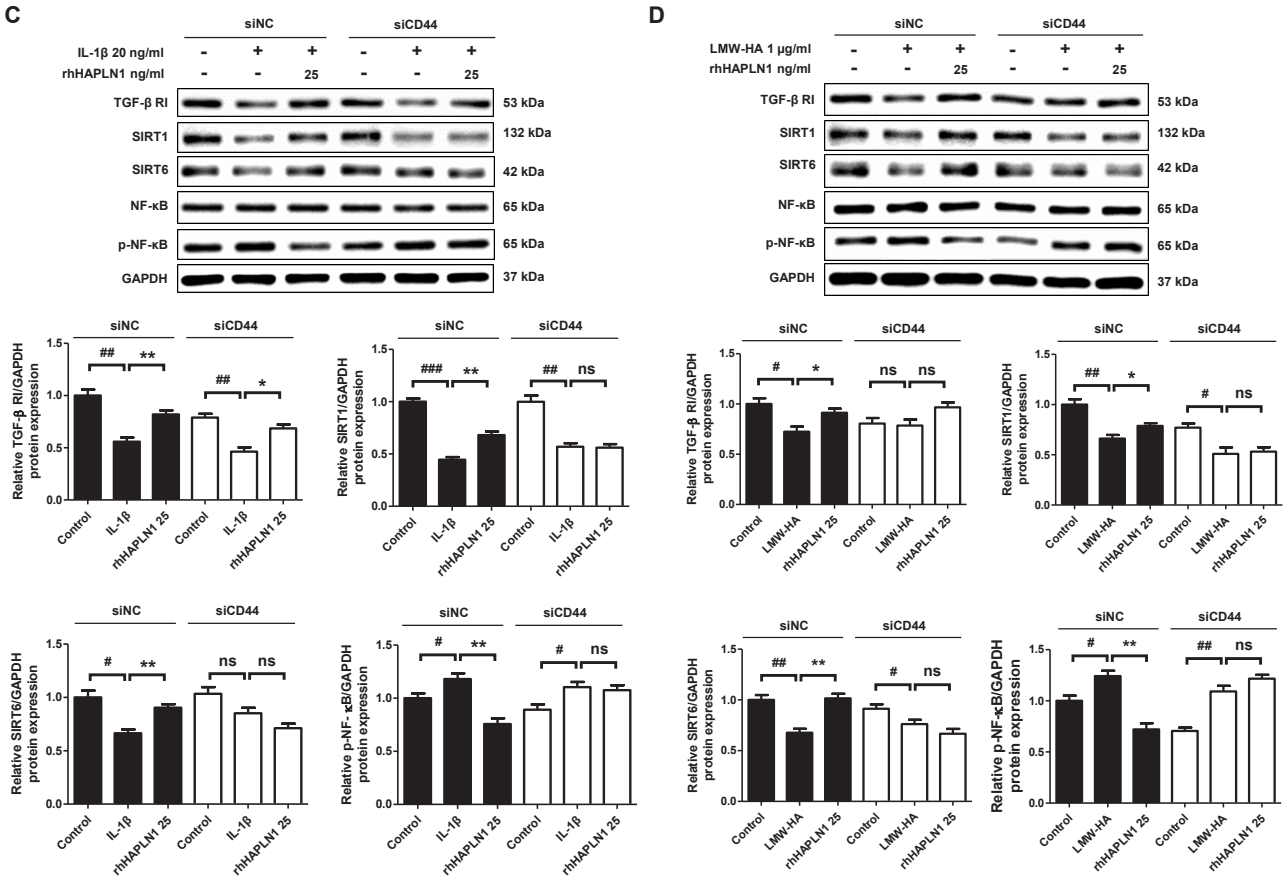

Fig. 3. Continued.

injection, followed by H&E staining of samples obtained from young and aged mice. We observed a significant alveolar recovery in the lung tissues of aged mice treated with rhHAPLN1 based on mean linear intercept (MLI), a measurement of alveolar/air space size, as a marker of emphysema (Fig. 4), indicating that rhHAPLN1 might reverse aging-driven enlargement of the alveolar spaces observed in aged mice.

rhHAPLN1 reduced significantly the length of MLI of alveoli as an indicative of the mouse PPE-induced COPD model

Intratracheal PPE administration resulted in a dose-dependent increase in emphysema (Khedoe et al., 2013). Accordingly, we established a disease model to investigate the action of rhHAPLN1 in alveolar damage caused by PPE. To investigate the protective effect of rhHAPLN1 on the damaged lungs, we assessed the lungs of the young C57BL/6N mice whose airways were exposed to PPE. We evaluated the impact of PPE on alveolar morphology using H&E staining. We utilized MLI to assess alveolar phenotypes associated with lung air space enlargement (Shimoyama et al., 2022). Our results showed that rhHAPLN1 significantly suppressed the enlargement caused by PPE based on the MLI values (Fig. 5A). Meanwhile, it has been demonstrated that HA can limit air cavity enlargement and prevent elastic fiber damage, supporting clinical trials in patients with clear existing evidence of COPD (Cantor et al., 2011). Therefore, HA was administered using an aerosol chamber and compared with rhHAPLN1 (Figs. 5A and 5B). Our results revealed that when rhHAPLN1 was administrated at ~17-fold lower dose by weight than HA, rhHAPLN1 showed ~95% recovery in the alveolar spatial enlargement in comparison to ~73% recovery for HA. Based on the concentration of rhHAPLN1 in Fig. 5A, low and high concentrations were tested (Figs. 5C and 5D). As a result, a significant MLI decrease was shown at high concentrations, but no effect was seen at low concentrations.

DISCUSSION

This study is the first to demonstrate a therapeutic effect of full-length HAPLN1 on PPE-induced emphysema as a COPD model and the underlying mechanisms. In our previous study, Fu et al. uncovered that rhHAPLN1 might rejuvenate aged skin by promoting the production of collagen I and HA from human dermal fibroblasts through the constitutive elevation of TGF-β RII, leading to the activation of both Smad2 and Smad3 by TGF-β1. In contrast, our present study demonstrated that the HAECs treated with rhHAPLN1 showed a selective enhancement of TGF-β RI, which led to a selective activation of Smad3 without TGF-β1 (Fig. 1). Also, such selective increase in TGF-β RII or TGF-β RI levels by rhHAPLN1 is CD44-dependent and occurs constitutively without TGF-β1. More importantly, our present results show that the selective

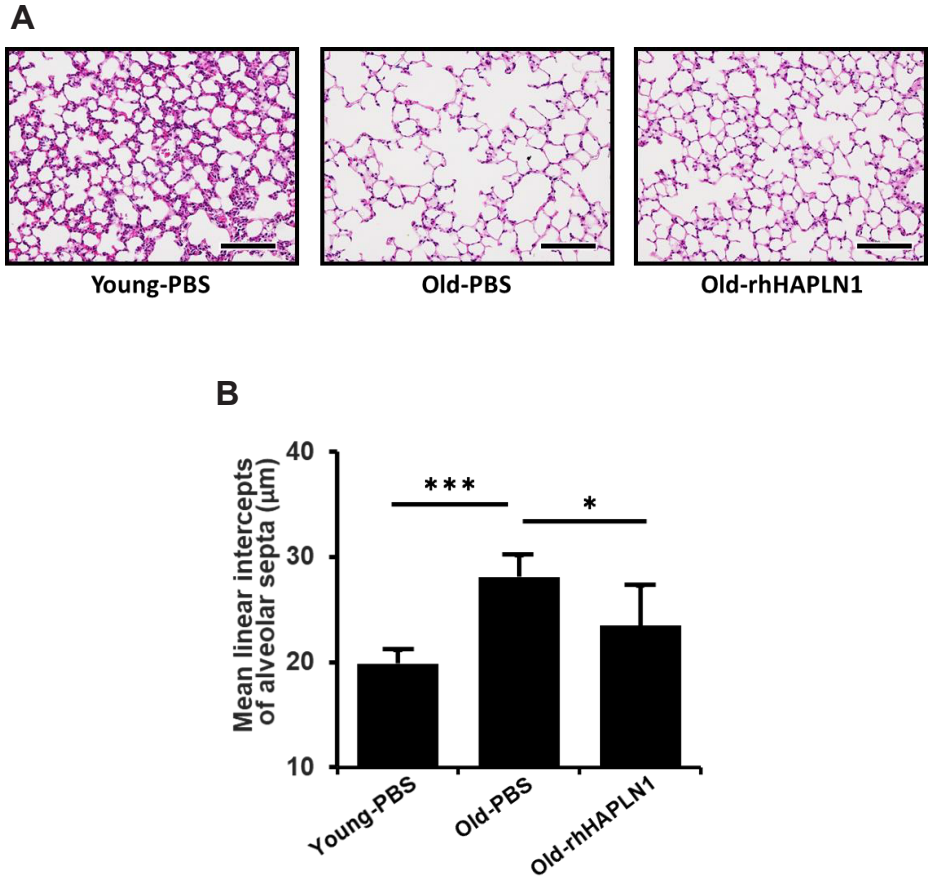

Fig. 4. rhHAPLN1 reduced significantly the length of MLI of alveoli as an indicative of the mouse senile emphysema. Five young male C57BL/6J mice aged 6 to 10 weeks and two groups of five old male mice aged 19 to 20 months were used. Young mice and one group of old mice were treated with phosphate-buffered saline (PBS) as Control groups. One group of the old mice was intraperitoneally injected with rhHAPLN1 (0.1 mg/kg) in PBS once every three days for nine times and then euthanized after 1 day of the final injection. The lungs were harvested, parasagittal sectioned, immersed in formalin, and paraffin blocks were made. The lung tissues were cut into 5 μm and stained with H&E. (A) Pictures of representative histological sections of the lungs were taken with a 200× optical microscope. (B) MLI (mean ± SEM) of alveolar septae were measured in the lungs of five young mice, the control group of five old mice, and rhHAPLN1-treated group of five old mice. The Stitcher ImageJ plugin program was used (Preibisch et al., 2009). $*P < 0.05$, $***P < 0.001$. Scale bars = 100 μm. rhHAPLN1, recombinant human hyaluronan and proteoglycan link protein 1; MLI, mean linear intercepts.

activation of Smad3 leads to the expression of SIRT1 and further suppresses the production of MMP9. This is consistent with previous studies, where it has been postulated that the Smad3 activation-mediated expression of SIRT1 epigenetically regulates MMP9 transcription, thus playing an essential role in modulating both emphysema and pulmonary fibrosis (Lee et al., 2021; Warburton et al., 2013; Xu et al., 2012). Accordingly, our findings support the missing link between TFG-β signaling and MMP9-induced alveolar destruction and the possibility that rhHAPLN1 can alleviate both pulmonary diseases. In an expansion of this study, most notably, we have also revealed that inhaled administration of rhHAPLN1-containing aerosols exhibited an extremely potent therapeutic efficacy in bleomycin-induced pulmonary fibrosis in mice, similar to that in the PPE-induced mouse COPD model (data not shown). Assumably, these observations seem to support the "Goldilocks hypothesis" for TGF-β-Smad signal transduction conceptualized and proposed by Shi et al. (2009), indicating that lack of TGF-β signaling results in abnormal lung alveolarization during development, whereas excessive amounts of TGF-β signaling causes fibrosis in the mature lung. Thus, these findings and this concept suggest that rhHAPLN1 has to be 'just right' for TGF-β signaling exerting its repairing effects on damaged lung tissues in both pulmonary diseases.

In our previous study using human dermal fibroblasts, blocking CD44 endocytosis or slowing its rate prevents the degradation of a large complex composed of aggregates, CD44, and tethered receptor, TGF-β RII. In contrast, in this study, CD44 seems to protect TGF-β RI in a similar fashion, although the precise mechanism by which rhHAPLN1 increases the levels of TGF-β receptors in a cell type-specific manner remains further investigated. Such a proposal could be deduced from the observation that the aggregate formed in the presence of HAPLN1, termed 'HAPLN1-containing

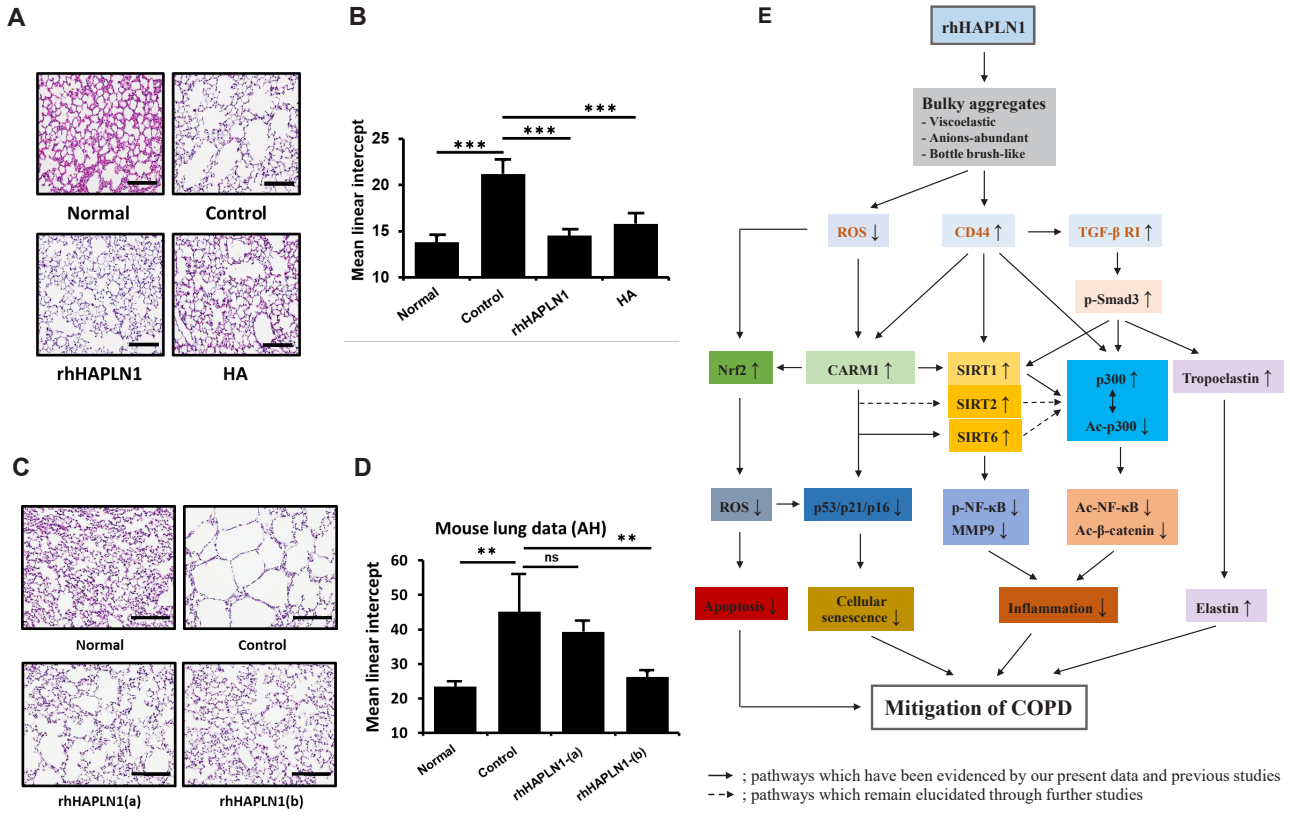

Fig. 5. rhHAPLN1 reduced significantly the length of MLI of alveoli as an indicator of the mouse PPE-induced COPD model. Male C57BL6/N mice aged 6 to 10 weeks were used as the experimental model. Mice were divided into four groups with six mice in each group in each of two independent experiments. In the 1st experiment, the groups were Normal, Control, rhHAPLN1 (0.00033% w/v), and high molecular weight hyaluronan (HMW-HA) groups (0.0057% w/v) (A and B), and in the 2nd experiment, groups were Normal, Control, rhHAPLN1-(a) (0.0001% w/v), and rhHAPLN1-(b) (0.0005% w/v) (C and D). In each experiment, to induce COPD in the three groups except Normal, on the day before the exposure to the test samples, PPE (30 μl/6 Unit/time) was injected into the oral airway with a 0.9 mm × 50 mm-oral zonde as a method of alveolar inhalation, and rhHAPLN1 or HMW-HA solubilized in vehicle saline was administered on the second day for 1 h daily and five times per week for 21 days, and then mice were euthanized after 1 day of the final exposure. The lungs were harvested, parasagittal sectioned, immersed in formalin, and paraffin blocks were made. The lung tissues were cut into 5 μm and stained with H&E. Pictures of representative histological sections of lungs were taken with a 200× optical microscope (A and C). MLI (mean ± SEM) of alveolar septae were measured in the lungs of six Normal mice, Control group of six saline-treated mice, and the rhHAPLN1-treated group of six mice. The Stitcher ImageJ plugin program was used (Preibisch et al., 2009) (B and D). Compared with those of each Control group, the results from 1st experiment showed that rhHAPLN1 significantly reduced the enlargement of alveoli as an indicative of emphysema: 0.00033% rhHAPLN1 group by 95% [(21.2 - 13.8)/21.2 - 14.5) × 100]; 0.0057% HMW-HA by 73.0% [(21.2 - 13.8)/21.2 - 15.8) × 100] (B), while 2nd experiment showed 0.0001% rhHAPLN1-(a) by no significance; 0.0005% rhHAPLN1-(b) by 87% [(45.1 - 26.2)/(45.1 - 23.4) × 100] (D). $*P < 0.05$, $**P < 0.01$, $***P < 0.001$. ns, no significance. Scale bars = 100 μm. (E) A proposed model showing a cross-talk between HAPLN1, CD44, TGF-β signaling, CARM1, sirtuins (SIRT1/2/6), and p300 for explaining the rhHAPLN1-mediated mitigation of COPD. Arrow lines indicate pathways which have been evidenced by our present data and previous studies; arrow dashed lines indicate pathways which remain elucidated through further studies. rhHAPLN1, recombinant human hyaluronan and proteoglycan link protein 1; MLI, mean linear intercepts; PPE, porcine pancreatic elastase; COPD, chronic obstructive pulmonary disease; HA, hyaluronan; ROS, reactive oxygen species; TGF-β RI, transforming growth factor β receptor 1; p-Smad3, phosphorylated Smad3; Nrf2, nuclear factor erythroid 2-related factor 2; CARM1, co-activator-associated arginine methyltransferase-1; Ac-p300, acetylated p300; p-NF-κB, phosphorylated NF-κB; MMP9, metalloproteinase-9.

aggregate', is five times longer and has three times more proteoglycans compared with HAPLN1-free aggregate because the former leads to increased stability of the linking between proteoglycans and HA (Buckwalter et al., 1984). The HAPLN1-containing aggregates have been proposed as a crucial mechanochemical signal transducer owing to their highly viscoelastic properties, thereby slowing the rate of HA-mediated CD44 internalization (Batchelder and Yarar, 2010; Danielson et al., 2015). At this point, it is conceivable to speculate that the high viscoelasticity of the HAPLN1-containing aggregate could influence CD44 clustering (Takasugi et al., 2020) and HA chain cross-linking (Day and de la Motte, 2005), thereby blocking or slowing its rate of endocytosis. A recent study demonstrates that the knockdown of CARM1 in lung epi-

thelial cells led to decreased SIRT1 expression but increased p16 and p21, suggesting that CARM1 suppresses alveolar senescence and emphysema upstream of SIRT1 (Sarker et al., 2015). Consistent with this study, our results showed that PPE- and H_2O_2-induced decreases in CARM1, and SIRT1, SIRT2, and SIRT6 levels were significantly reversed by rhHAPLN1 (Figs. 2A and 2B), and interestingly, knockdown of CARM1 remarkably diminished the rescue effect of rhHAPLN1 on SIRT1 and SIRT6 (Fig. 2B), suggesting that CARM1 may be an important upstream regulator for such protective effectors. Meanwhile, knockdown of CD44 also abolished the rescue effect of rhHAPLN1 on SIRT1 and SIRT6 (Fig. 3B). These findings suggest that CD44 and/or CARM1 may be required for increases in SIRT1 and SIRT6 levels. Although a recent review proposes that CD44 may upregulate the SIRT1 levels via PI3K/Akt pathway, they do not provide direct evidence for CD44-mediated regulation of SIRT1 (Ahmad et al., 2022). In this context, it is worth noting that PI3K-Akt-GSK3β signaling pathway is required for SIRT1 induction by ER stress (Koga et al., 2015) and HMW-HA-CD44 interaction has been shown to promote proliferation of decidual cells during the early stages of pregnancy by activating the PI3K/Akt (Zhu et al., 2013). Accordingly, along with these previous findings, our results imply that rhHAPLN1 could upregulate SIRT1 expression via the HA-CD44-mediated PI3K/Akt pathway and/or CARM1 pathway different from the p-Smad3 pathway as previously addressed (Warburton et al., 2013). Notably, despite knockdown of CARM1, rhHAPLN1 partly rescued the SIRT6 levels decreased by H_2O_2, suggesting a lack of relationship between CARM1 and SIRT6. Further studies are required to clarify this issue since previous studies have indicated that SIRT1 acts epigenetically on the SIRT6 promoter and positively regulates expression of SIRT6 (Calvanese et al., 2010; Kim et al., 2010). In contrast, such CD44-dependent rescue effect of rhHAPLN1 on SIRT1 and SIRT6 levels might result from certain different pathway via HA-CD44 interactions; namely, it will be noteworthy that HA-CD44 interactions inhibit SIRT1 deacetylase activity by activating p300 acetyltransferase activity (Bourguignon et al., 2009). In contrast, SIRT1 induces deacetylation and repression of p300 transactivation through direct physical interaction, requiring the NAD-dependent deacetylase activity of SIRT1 (Bouras et al., 2005). Therefore, HA-CD44 interactions increase p300 activity by inhibiting SIRT1 activation (Bourguignon et al., 2009), and TGF-β signaling upregulates the expression of p300 (Bhattacharyya et al., 2005), suggesting that both pathways could promote the acetylation of β-catenin and NF-κB (Lee et al., 2021). These prior findings suggest that the interplay between HA-CD44-stimulated p300 activation and p-smad3-activated SIRT1 expression plays pivotal roles in regulating the balance between cell survival and apoptosis in cells. In this context, our results showing the rhHAPLN1-induced decrease in the levels of the active form of Ac-p300 provide important insights into the mechanism by which rhHAPLN1 upregulates the levels of SIRT1 via the HA-CD44-p300 axis besides canonical TGF-β1-p-Smad3 signaling (Fig. 1C, lane 5).

In contrast, it has been reported that nuclear co-regulators p300 and CARM1 can transactivate Nrf2 (Lin et al., 2006), which is known to represent an essential break in the vicious cycle that prevents exacerbated inflammation and subsequent tissue damage through a critical role in scavenging ROS (Cuadrado et al., 2019; Lee et al., 2022). Given that rhHAPLN1 inhibited TGF-β1–mediated p300 activation, the interplay between p300 and CARM1 will be an interesting issue for the rhHAPLN1-induced increase in Nrf2 levels. Nonetheless, our results consequently showed that rhHAPLN1 rescued Nrf2 levels decreased by H_2O_2 in the siNC group but not in the CARM1-knockdown group (Fig. 2B) and reversed the ROS levels increased by various cell-damaged insults, including H_2O_2, PPE, IL-1β, and LMW-HA (Fig. 2C), prompting us to investigate whether cellular senescence and inflammation can also be regulated by rhHAPLN1. Our results revealed that rhHAPLN1 decreased the levels of p53, p21, and p16 increased by PPE (Figs. 2D and 2E). Furthermore, our results showed that rhHAPLN1 suppressed the p-NF-κB levels in a CD44-dependent manner with concurrent increases in TGF-β RI and SIRT1 and SIRT6 levels. Taken together, our findings strongly imply a therapeutic efficacy against pulmonary emphysema owing to such potent anti-senescent and anti-inflammatory effects at sub-nanomolar concentrations. More importantly our *in vivo* results indicated that both senile emphysema mouse model, induced via the intraperitoneal injection of rhHAPLN1, and PPE-induced COPD mouse model, generated via inhaled administrations of rhHAPLN1-containing aerosols, showed an extremely potent efficacy in reducing the enlargements of alveolar spaces. Currently, preclinical trials are underway to study the effects of inhaled rhHAPLN1-containing aerosols on several COPD animal models. Therefore, rhHAPLN1 could be a potential therapeutic solution for pulmonary emphysema.

In summary, in our previous work, the application of parabiosis-based and aptamer-based proteomic studies explained some fundamental questions regarding the systemic regulation of skin aging. In an expansion of that study, here, we demonstrate that rhHAPLN1 can prevent and even reverse the aging- and environmental factor-related decline in the integrity of the alveolar wall. This therapeutic efficacy likely results from the mechanism by which rhHAPLN1 increases TGF-β RI levels from possibly its endocytic degradation at the cell surface in a CD44-dependent manner and protects alveolar epithelial cells from destructive damages by regulating CARM1, sirtuins like SIRT1/2/6, Nrf2, and NF-κB, leading to anti-senescent and anti-inflammatory effects. Collectively, we propose a model showing a cross-talk between rhHAPLN1, CD44, TGF-β signaling, CARM1, sirtuins (SIRT1/2/6), and p300 for explaining the rhHAPLN1-mediated mitigation of COPD (Fig. 5E). Currently, preclinical trials are underway to study the effects of inhaled rhHAPLN1-containing aerosols in several COPD animal models as well as idiopathic pulmonary fibrosis animal models.

Note: Supplementary information is available on the Molecules and Cells website (www.molcells.org).

ACKNOWLEDGMENTS

This study was supported by the National Research Foundation of Korea grant (NRF-2017M3A9D8048414) funded by the Korean Government (Ministry of Science and ICT). We

thank Dr. Eui Man Jeong (College of Pharmacy, Jeju National University, Republic of Korea) for discussion and interpretation on reactive oxygen species.

AUTHOR CONTRIBUTIONS

The overall study was designed by Y.P., H.H.K., and D.K.K. D.K.K. also supervised the study. Y.P., S.Y.Y., and Z.F. performed the *in vitro* experiments. Y.P., J.M.J., and M.J.B. performed the *in vivo* experiments. Y.P. and D.K.K. drafted the paper. All authors discussed the results and implications and commented on the manuscript.

CONFLICT OF INTEREST

Y.P., S.Y.Y., Z.F., and J.M.J. are employees of HapInScience Inc. M.J.B. was employee of HapInScience Inc. J.M.J., H.H.K., and D.K.K. are shareholders of HapInScience Inc. D.K.K. is the chief science officer of HapInScience Inc. None of the authors have conflicts of interest to declare.

HapInScience currently holds a patent for the use of HAPLN1 in COPD conditions, with Y.P., S.Y.Y., J.M.J., and D.K.K. listed as inventors. The registration number is "1021664530000".

ORCID

Yongwei Piao https://orcid.org/0009-0005-2687-3314
So Yoon Yun https://orcid.org/0009-0007-0195-0680
Zhicheng Fu https://orcid.org/0000-0001-8337-3790
Ji Min Jang https://orcid.org/0000-0001-9071-3941
Moon Jung Back https://orcid.org/0009-0003-4545-0507
Ha Hyung Kim https://orcid.org/0000-0002-8891-4928
Dae Kyong Kim https://orcid.org/0009-0000-0388-7303

REFERENCES

Ahmad, S.M.S., Al-Mansoob, M., and Ouhtit, A. (2022). SIRT1, a novel transcriptional downstream target of CD44, linking its deacetylase activity to tumor cell invasion/metastasis. Front. Oncol. *12*, 1038121.

Baker, J.R., Vuppusetty, C., Colley, T., Papaioannou, A.I., Fenwick, P., Donnelly, L., Ito, K., and Barnes, P.J. (2016). Oxidative stress dependent microRNA-34a activation via PI3Kalpha reduces the expression of sirtuin-1 and sirtuin-6 in epithelial cells. Sci. Rep. *6*, 35871.

Barkauskas, C.E., Cronce, M.J., Rackley, C.R., Bowie, E.J., Keene, D.R., Stripp, B.R., Randell, S.H., Noble, P.W., and Hogan, B.L. (2013). Type 2 alveolar cells are stem cells in adult lung. J. Clin. Invest. *123*, 3025-3036.

Barnes, P.J. (2017). Senescence in COPD and its comorbidities. Annu. Rev. Physiol. *79*, 517-539.

Batchelder, E.M. and Yarar, D. (2010). Differential requirements for clathrin-dependent endocytosis at sites of cell-substrate adhesion. Mol. Biol. Cell *21*, 3070-3079.

Bhattacharyya, S., Ghosh, A.K., Pannu, J., Mori, Y., Takagawa, S., Chen, G., Trojanowska, M., Gilliam, A.C., and Varga, J. (2005). Fibroblast expression of the coactivator p300 governs the intensity of profibrotic response to transforming growth factor beta. Arthritis Rheum. *52*, 1248-1258.

Bouras, T., Fu, M., Sauve, A.A., Wang, F., Quong, A.A., Perkins, N.D., Hay, R.T., Gu, W., and Pestell, R.G. (2005). SIRT1 deacetylation and repression of p300 involves lysine residues 1020/1024 within the cell cycle regulatory domain 1. J. Biol. Chem. *280*, 10264-10276.

Bourguignon, L.Y., Singleton, P.A., Zhu, H., and Zhou, B. (2002). Hyaluronan promotes signaling interaction between CD44 and the transforming growth factor beta receptor I in metastatic breast tumor cells. J. Biol. Chem. *277*, 39703-39712.

Bourguignon, L.Y.W., Xia, W., and Wong, G. (2009). Hyaluronan-mediated CD44 interaction with p300 and SIRT1 regulates beta-catenin signaling and NFkappaB-specific transcription activity leading to MDR1 and Bcl-xL gene expression and chemoresistance in breast tumor cells. J. Biol. Chem. *284*, 2657-2671.

Buckley, S., Shi, W., Barsky, L., and Warburton, D. (2008). TGF-beta signaling promotes survival and repair in rat alveolar epithelial type 2 cells during recovery after hyperoxic injury. Am. J. Physiol. Lung Cell. Mol. Physiol. *294*, L739-L748.

Buckwalter, J.A., Rosenberg, L.C., and Tang, L.H. (1984). The effect of link protein on proteoglycan aggregate structure. An electron microscopic study of the molecular architecture and dimensions of proteoglycan aggregates reassembled from the proteoglycan monomers and link proteins of bovine fetal epiphyseal cartilage. J. Biol. Chem. *259*, 5361-5363.

Calvanese, V., Lara, E., Suarez-Alvarez, B., Abu Dawud, R., Vazquez-Chantada, M., Martinez-Chantar, M.L., Embade, N., Lopez-Nieva, P., Horrillo, A., Hmadcha, A., et al. (2010). Sirtuin 1 regulation of developmental genes during differentiation of stem cells. Proc. Natl. Acad. Sci. U. S. A. *107*, 13736-13741.

Cantor, J.O., Cerreta, J.M., Ochoa, M., Ma, S., Chow, T., Grunig, G., and Turino, G.M. (2005). Aerosolized hyaluronan limits airspace enlargement in a mouse model of cigarette smoke-induced pulmonary emphysema. Exp. Lung Res. *31*, 417-430.

Cantor, J.O., Cerreta, J.M., Ochoa, M., Ma, S., Liu, M., and Turino, G.M. (2011). Therapeutic effects of hyaluronan on smoke-induced elastic fiber injury: does delayed treatment affect efficacy? Lung *189*, 51-56.

Chen, H., Sun, J., Buckley, S., Chen, C., Warburton, D., Wang, X.F., and Shi, W. (2005). Abnormal mouse lung alveolarization caused by Smad3 deficiency is a developmental antecedent of centrilobular emphysema. Am. J. Physiol. Lung Cell. Mol. Physiol. *288*, L683-L691.

Isacke, C.M. and Yarwood, H. (2002). The hyaluronan receptor, CD44. Int. J. Biochem. Cell Biol. *34*, 718-721.

Cuadrado, A., Rojo, A.I., Wells, G., Hayes, J.D., Cousin, S.P., Rumsey, W.L., Attucks, O.C., Franklin, S., Levonen, A.L., Kensler, T.W., et al. (2019). Therapeutic targeting of the NRF2 and KEAP1 partnership in chronic diseases. Nat. Rev. Drug Discov. *18*, 295-317.

D'Onofrio, N., Servillo, L., and Balestrieri, M.L. (2018). SIRT1 and SIRT6 signaling pathways in cardiovascular disease protection. Antioxid. Redox Signal. *28*, 711-732.

Danielson, B.T., Knudson, C.B., and Knudson, W. (2015). Extracellular processing of the cartilage proteoglycan aggregate and its effect on CD44-mediated internalization of hyaluronan. J. Biol. Chem. *290*, 9555-9570.

Day, A.J. and de la Motte, C.A. (2005). Hyaluronan cross-linking: a protective mechanism in inflammation? Trends Immunol. *26*, 637-643.

Desai, T.J., Brownfield, D.G., and Krasnow, M.A. (2014). Alveolar progenitor and stem cells in lung development, renewal and cancer. Nature *507*, 190-194.

Garantziotis, S. and Savani, R.C. (2019). Hyaluronan biology: a complex balancing act of structure, function, location and context. Matrix Biol. *78-79*, 1-10.

Harada, H. and Takahashi, M. (2007). CD44-dependent intracellular and extracellular catabolism of hyaluronic acid by hyaluronidase-1 and -2. J. Biol. Chem. *282*, 5597-5607.

Harman, D. (2006). Free radical theory of aging: an update: increasing the functional life span. Ann. N. Y. Acad. Sci. *1067*, 10-21.

Hou, H.H., Cheng, S.L., Liu, H.T., Yang, F.Z., Wang, H.C., and Yu, C.J. (2013). Elastase induced lung epithelial cell apoptosis and emphysema through placenta growth factor. Cell Death Dis. *4*, e793.

Ito, K. and Barnes, P.J. (2009). COPD as a disease of accelerated lung aging. Chest *135*, 173-180.

Jain, R., Barkauskas, C.E., Takeda, N., Bowie, E.J., Aghajanian, H., Wang, Q., Padmanabhan, A., Manderfield, L.J., Gupta, M., Li, D., et al. (2015). Plasticity of Hopx(+) type I alveolar cells to regenerate type II cells in the lung. Nat. Commun. *6*, 6727.

Jiang, D., Liang, J., Fan, J., Yu, S., Chen, S., Luo, Y., Prestwich, G.D., Mascarenhas, M.M., Garg, H.G., Quinn, D.A., et al. (2005). Regulation of lung injury and repair by Toll-like receptors and hyaluronan. Nat. Med. *11*, 1173-1179.

Kato, R., Mizuno, S., Kadowaki, M., Shiozaki, K., Akai, M., Nakagawa, K., Oikawa, T., Iguchi, M., Osanai, K., Ishizaki, T., et al. (2016). Sirt1 expression is associated with CD31 expression in blood cells from patients with chronic obstructive pulmonary disease. Respir. Res. *17*, 139.

Khedoe, P.P., Wong, M.C., Wagenaar, G.T., Plomp, J.J., van Eck, M., Havekes, L.M., Rensen, P.C., Hiemstra, P.S., and Berbee, J.F. (2013). The effect of PPE-induced emphysema and chronic LPS-induced pulmonary inflammation on atherosclerosis development in APOE*3-LEIDEN mice. PLoS One *8*, e80196.

Kim, H.S., Xiao, C., Wang, R.H., Lahusen, T., Xu, X., Vassilopoulos, A., Vazquez-Ortiz, G., Jeong, W.I., Park, O., Ki, S.H., et al. (2010). Hepatic-specific disruption of SIRT6 in mice results in fatty liver formation due to enhanced glycolysis and triglyceride synthesis. Cell Metab. *12*, 224-236.

Kirkil, G., Hamdi Muz, M., Seckin, D., Sahin, K., and Kucuk, O. (2008). Antioxidant effect of zinc picolinate in patients with chronic obstructive pulmonary disease. Respir. Med. *102*, 840-844.

Koga, T., Suico, M.A., Shimasaki, S., Watanabe, E., Kai, Y., Koyama, K., Omachi, K., Morino-Koga, S., Sato, T., Shuto, T., et al. (2015). Endoplasmic reticulum (ER) stress induces sirtuin 1 (SIRT1) expression via the PI3K-Akt-GSK3beta signaling pathway and promotes hepatocellular injury. J. Biol. Chem. *290*, 30366-30374.

Königshoff, M., Kneidinger, N., and Eickelberg, O. (2009). TGF-beta signaling in COPD: deciphering genetic and cellular susceptibilities for future therapeutic regimens. Swiss Med. Wkly. *139*, 554-563.

Lee, J.A., Kwon, Y.W., Kim, H.R., Shin, N., Son, H.J., Cheong, C.S., Kim, D.J., and Hwang, O. (2022). A novel pyrazolo[3,4-d]pyrimidine induces heme oxygenase-1 and exerts anti-inflammatory and neuroprotective effects. Mol. Cells *45*, 134-147.

Lee, S.U., Kim, M.O., Kang, M.J., Oh, E.S., Ro, H., Lee, R.W., Song, Y.N., Jung, S., Lee, J.W., Lee, S.Y., et al. (2021). Transforming growth factor beta inhibits MUC5AC expression by Smad3/HDAC2 complex formation and NF-kappaB deacetylation at K310 in NCI-H292 cells. Mol. Cells *44*, 38-49.

Liang, G.B. and He, Z.H. (2019). Animal models of emphysema. Chin. Med. J. (Engl.) *132*, 2465-2475.

Lin, W., Shen, G.X., Yuan, X.L., Jain, M.R., Yu, S.W., Zhang, A.H., Chen, J.D., and Kong, A.N.T. (2006). Regulation of Nrf2 transactivation domain activity by p160 RAC3/SRC3 and other nuclear co-regulators. J. Biochem. Mol. Biol. *39*, 304-310.

Liu, R., Hao, D., Xu, W., Li, J., Li, X., Shen, D., Sheng, K., Zhao, L., Xu, W., Gao, Z., et al. (2019). beta-Sitosterol modulates macrophage polarization and attenuates rheumatoid inflammation in mice. Pharm. Biol. *57*, 161-168.

Mebratu, Y.A., Smith, K.R., Agga, G.E., and Tesfaigzi, Y. (2016). Inflammation and emphysema in cigarette smoke-exposed mice when instilled with poly (I:C) or infected with influenza A or respiratory syncytial viruses. Respir. Res. *17*, 75.

Mercado, N., Ito, K., and Barnes, P.J. (2015). Accelerated ageing of the lung in COPD: new concepts. Thorax *70*, 482-489.

Misra, S., Hascall, V.C., Markwald, R.R., and Ghatak, S. (2015). Interactions between hyaluronan and its receptors (CD44, RHAMM) regulate the activities of inflammation and cancer. Front. Immunol. *6*, 201.

Murray, C.J. and Lopez, A.D. (2013). Measuring the global burden of disease. N. Engl. J. Med. *369*, 448-457.

Nakamaru, Y., Vuppusetty, C., Wada, H., Milne, J.C., Ito, M., Rossios, C., Elliot, M., Hogg, J., Kharitonov, S., Goto, H., et al. (2009). A protein deacetylase SIRT1 is a negative regulator of metalloproteinase-9. FASEB J. *23*, 2810-2819.

Ouhtit, A., Gaur, R.L., Abdraboh, M., Ireland, S.K., Rao, P.N., Raj, S.G., Al-Riyami, H., Shanmuganathan, S., Gupta, I., Murthy, S.N., et al. (2013). Simultaneous inhibition of cell-cycle, proliferation, survival, metastatic pathways and induction of apoptosis in breast cancer cells by a phytochemical super-cocktail: genes that underpin its mode of action. J. Cancer *4*, 703-715.

Paschalaki, K.E., Starke, R.D., Hu, Y., Mercado, N., Margariti, A., Gorgoulis, V.G., Randi, A.M., and Barnes, P.J. (2013). Dysfunction of endothelial progenitor cells from smokers and chronic obstructive pulmonary disease patients due to increased DNA damage and senescence. Stem Cells *31*, 2813-2826.

Patel, B.D., Loo, W.J., Tasker, A.D., Screaton, N.J., Burrows, N.P., Silverman, E.K., and Lomas, D.A. (2006). Smoking related COPD and facial wrinkling: is there a common susceptibility? Thorax *61*, 568-671.

Preibisch, S., Saalfeld, S., and Tomancak, P. (2009). Globally optimal stitching of tiled 3D microscopic image acquisitions. Bioinformatics *25*, 1463-1465.

Rahman, I., Kinnula, V.L., Gorbunova, V., and Yao, H. (2012). SIRT1 as a therapeutic target in inflammaging of the pulmonary disease. Prev. Med. *54* Suppl, S20-S28.

Rajendrasozhan, S., Yang, S.R., Kinnula, V.L., and Rahman, I. (2008). SIRT1, an antiinflammatory and antiaging protein, is decreased in lungs of patients with chronic obstructive pulmonary disease. Am. J. Respir. Crit. Care Med. *177*, 861-870.

Rodriguez-Castillo, J.A., Perez, D.B., Ntokou, A., Seeger, W., Morty, R.E., and Ahlbrecht, K. (2018). Understanding alveolarization to induce lung regeneration. Respir. Res. *19*, 148.

Roughley, P.J., Poole, A.R., and Mort, J.S. (1982). The heterogeneity of link proteins isolated from human articular cartilage proteoglycan aggregates. J. Biol. Chem. *257*, 11908-11914.

Sarker, R.S., John-Schuster, G., Bohla, A., Mutze, K., Burgstaller, G., Bedford, M.T., Konigshoff, M., Eickelberg, O., and Yildirim, A.O. (2015). Coactivator-associated arginine methyltransferase-1 function in alveolar epithelial senescence and elastase-induced emphysema susceptibility. Am. J. Respir. Cell Mol. Biol. *53*, 769-781.

Sarker, R.S.J., Conlon, T.M., Morrone, C., Srivastava, B., Konyalilar, N., Verleden, S.E., Bayram, H., Fehrenbach, H., and Yildirim, A.O. (2019). CARM1 regulates senescence during airway epithelial cell injury in COPD pathogenesis. Am. J. Physiol. Lung Cell. Mol. Physiol. *317*, L602-L614.

Shi, W., Xu, J., and Warburton, D. (2009). Development, repair and fibrosis: what is common and why it matters. Respirology *14*, 656-665.

Shimoyama, T., Kaneda, M., Yoshida, S., Michihara, S., Fujita, N., Han, L.K., and Takahashi, R. (2022). Ninjin'yoeito ameliorated PPE-induced pulmonary emphysema and anxiety/depressive-like behavior in aged C57BL/6J mice. Front. Pharmacol. *13*, 970697.

Sorokin, L. (2010). The impact of the extracellular matrix on inflammation. Nat. Rev. Immunol. *10*, 712-723.

Takasugi, M., Firsanov, D., Tombline, G., Ning, H., Ablaeva, J., Seluanov, A., and Gorbunova, V. (2020). Naked mole-rat very-high-molecular-mass hyaluronan exhibits superior cytoprotective properties. Nat. Commun. *11*, 2376.

Vomund, S., Schafer, A., Parnham, M.J., Brune, B., and von Knethen, A. (2017). Nrf2, the master regulator of anti-oxidative responses. Int. J. Mol. Sci. *18*, 2772.

Warburton, D., Shi, W., and Xu, B. (2013). TGF-beta-Smad3 signaling in emphysema and pulmonary fibrosis: an epigenetic aberration of normal

development? Am. J. Physiol. Lung Cell. Mol. Physiol. *304*, L83-L85.

Xu, B., Chen, H., Xu, W., Zhang, W., Buckley, S., Zheng, S.G., Warburton, D., Kolb, M., Gauldie, J., and Shi, W. (2012). Molecular mechanisms of MMP9 overexpression and its role in emphysema pathogenesis of Smad3-deficient mice. Am. J. Physiol. Lung Cell. Mol. Physiol. *303*, L89-L96.

Yanagisawa, S., Papaioannou, A.I., Papaporfyriou, A., Baker, J.R., Vuppusetty, C., Loukides, S., Barnes, P.J., and Ito, K. (2017). Decreased serum sirtuin-1 in COPD. Chest *152*, 343-352.

Yao, H., Chung, S., Hwang, J.W., Rajendrasozhan, S., Sundar, I.K., Dean, D.A., McBurney, M.W., Guarente, L., Gu, W., Ronty, M., et al. (2012). SIRT1 protects against emphysema via FOXO3-mediated reduction of premature senescence in mice. J. Clin. Invest. *122*, 2032-2045.

Yi, J. and Luo, J. (2010). SIRT1 and p53, effect on cancer, senescence and beyond. Biochim. Biophys. Acta *1804*, 1684-1689.

Yu, M., Zhang, H., Wang, B., Zhang, Y., Zheng, X., Shao, B., Zhuge, Q., and Jin, K. (2021). Key signaling pathways in aging and potential interventions for healthy aging. Cells *10*, 660.

Zhang, M., An, C., Gao, Y., Leak, R.K., Chen, J., and Zhang, F. (2013). Emerging roles of Nrf2 and phase II antioxidant enzymes in neuroprotection. Prog. Neurobiol. *100*, 30-47.

Zhu, R., Wang, S.C., Sun, C., Tao, Y., Piao, H.L., Wang, X.Q., Du, M.R., and Li, D.J. (2013). Hyaluronan-CD44 interaction promotes growth of decidual stromal cells in human first-trimester pregnancy. PLoS One *8*, e74812.

Zhu, R.Z., Li, B.S., Gao, S.S., Seo, J.H., and Choi, B.M. (2021). Luteolin inhibits H(2)O(2)-induced cellular senescence via modulation of SIRT1 and p53. Korean J. Physiol. Pharmacol. *25*, 297-305.